A theoretical criterion to determine the appropriate tracking strategy for PV solar systems

D. R. Rousse, G. Quesada, L. Guillon,
P.L. Paradis, M. Mehrtash and Yvan Dutil

t3e Industrial Research Chair, École de Technologie Supérieure, Canada. daniel@t3e.info

Abstract:
Several papers indicate that fixed PV systems recover about 20% to 50% less solar energy than solar tracking photovoltaic (PV) systems. Despite these results, some recent studies propose to set the PV modules toward the zenith (fixed horizontal position) on overcast or cloudy days. This strategy is believed to increase the recovered solar radiation – and subsequently the overall electricity production – as compared with a system that simply follows the sun's path. This work focuses on the hourly and seasonally evaluation of this strategy for a solar tracking PV panel operating in Canada. A theoretical method based on the isotropic sky model was formulated, implemented, and used in a case study analysis of a grid connected PV system located in Toronto, Ontario. The results obtained, based on the definition of a critical hourly global solar radiation, were validated by use of a commercial software for design and analysis of PV systems. The case study analysis confirmed the disadvantage of the sun tracking strategy for overcast or mostly cloudy days in summer. However, in winter, the reflected radiation from the snow on the ground could increase the incident solar radiation upon tracking PV panels. Consequently, a tilted position could be more efficient than the horizontal one in such conditions.

Keywords: Solar Energy, Photovoltaic, Solar Tracker, Tracking Strategies, Albedo.

1. Introduction

It has been demonstrated that tracking the sun with solar panels largely increases the average yearly energy production with respect to panels set in a fixed position [1]. Nevertheless, because in overcast or cloudy conditions more than 90% of the solar radiation may be diffused [2], tracking the sun could be ineffective as the albedo of the environment is generally lower than that of the clouded sky itself. Hence, in partially cloudy conditions, as a function of the clearness index, tracking the sun could be either effective or unnecessary. Knowing for which conditions it is more advantageous to track the sun is an important issue for the optimisation of the operation of solar panels under any climatic conditions. But this is especially relevant under Canadian weather conditions as the presence of snow, both on the ground and on the panel itself, influences the performance.

Under cloudy conditions, normally a low amount of energy is produced. Hence, studies of the tracking strategy optimization under cloudy conditions are sparse and are relatively recent. The oldest reported work on this topic is a study carried out about 20 years ago by Appelbaum et al. [3] on the performance of solar arrays on Mars. While there are no significant clouds on Mars, dusty atmospheric conditions are somewhat similar to an overcast sky on Earth. This theoretical study demonstrated that in dusty conditions (optically thick atmosphere) dual axis tracking and horizontal surfaces provided almost the same power. Later, Badescu [4] created a more refined model for the PV cells working under Martian conditions. He also concluded that there is little difference between the electrical power output of the PV array when different strategies (horizontally oriented, south-facing tilted and dual axis tracking) are considered to collect solar radiation, mainly consisting of diffuse radiation. However, it is the seminal work of Kelly and Gibson [5] which is the best known starting point for the current research. The authors made measurements of the solar irradiance during cloudy periods. They measures solar irradiance on the horizontal position (G_H) and on a surface pointing directly towards the sun (G_{DTS}). The authors [5] suggested the following equation to define the tracking advantage (*TA*) of a dual-axis tracking panel versus a fixed horizontal panel:

$$TA = \frac{G_{DTS} - G_H}{G_H} = \frac{1 - \frac{G_H}{G_{DTS}}}{\frac{G_H}{G_{DTS}}} \tag{1}$$

Here the right-hand side of Eq.(1) is the original formulation of Kelly and Gibson [5] whereas it can be written more concisely as shown by the middle term. Although Eq.(1) is written in terms of power (instantaneous energy), in this study the concept will be extended to the energy recovered during a period of time.

Since all measurements were performed on overcast days, the authors obtained negative values for *TA* (a tracking disadvantage) ranging from -0.17 to -0.45 with an average of -0.31. These results led them [5] to conclude that orienting solar panels toward the zenith allows to capture more energy than with moving panels that simply track the sun’s path every day regardless of the sky conditions.

In a subsequent study, Kelly and Gibson [6] reported an extensive set of measurements for solar irradiance at noon. They used four identical PV solar arrays and associated silicon-photodiode pyranometers with different tilt angles (57°, 42°, 27° and 0°) relative to the earth’s surface. Their objective was to determine an optimal tracking algorithm for capturing solar radiation. The data was collected at Milford, Michigan (42°35' N). Over an overcast day, they estimated that the horizontal orientation of a PV panel can collect up to 50% more solar energy than a system that moves with the sun hidden behind the clouds..

Koussa et al. [7, 8, 9] studied the effect of eight different tracking configurations on the performance of solar PV panels. The evaluation was performed on the basis of hourly measurements of direct normal, horizontal global and diffuse solar radiation as well as the ambient temperature. Data was collected at Bouzareah (36°47' N) [8] and Ghardaïa location (32.4°N) [9], situated in the desert in the North of Algeria. A theoretical model was used to calculate the energy performance of each PV panel configuration. They reported that, during an overcast day, the horizontally oriented PV panel provides the best performance, compared to the other configurations.

Although the above mentioned papers indicate a disadvantage of sun tracking on cloudy days, none of them investigated the hourly and seasonal results as well as the influence of ground albedo on *TA*. The aim of this work is therefore to determine the best tracking strategy for a dual-axis tracking PV panel during cloudy conditions in high latitude locations. A secondary goal is to propose a simple yet efficient way to determine whether or not a PV panel should be set horizontally on cloudy days. To reach these goals, the available (incident) solar energy, on one hand, and the conversion of sunlight to electricity, on the other hand, have been investigated theoretically.The contribution of this paper lies in the formulation of a method to theoretically estimate the value of hourly solar energy incident on a horizontal surface for each day of the year below which it is more advantageous to set a dual-axis tracking PV panel in horizontal position.

The following section presents the concept of critical solar radiation and associated theory. This study involves all hours in day, several periods of the year and is not restricted to solar noon and a single day [6]. Then, the case study of a PV system located in Toronto, Canada, is simulated with PV-Sol Pro 4.5 to evaluate the relevance of this concept of critical solar radiation. In the 4th section, the recommended strategy is summarized while section 5 presents the concluding remarks. In [10], the authors apply the ideas developed herein in a city where measurements were carried out to confirm the usefulness of the proposed concept.

2. Critical solar radiation calculation

In an effort to propose a simple and yet accurate method to determine the best tracking strategy under cloudy conditions, this paper suggests a theoretical approach based on an isotropic sky model for any PV panel. This methodology estimates the theoretical value of global or integrated solar radiation incident on a horizontal plane under which a PV panel, horizontally oriented, receives and produces more energy than one following the sun. This value has been called "*critical hourly global solar radiation*" (I_c).

2.1. Solar radiation on a surface

The hourly global solar radiation on a tilted surface (I_T) is the sum of the direct beam ($I_{T,b}$), the sky-diffuse ($I_{T,d}$), and the ground reflected ($I_{T,r}$) integrated solar radiation on the surface,

$$I_T = I_{T,b} + I_{T,\mathrm{d}} + I_{T,r} \tag{2}$$

For an overcast or mostly cloudy sky, it is valid to use the isotropic sky model to assess the hourly global solar radiation upon a tilted surface (I_T) [11-12]. Hence, the diffuse radiation incident on a tilted surface comes diffusely from the fraction of the sky dome seen by it and from the diffuse reflection from the environment [13]. For the calculation of the ground reflected radiation incident on the tilted surface, the foreground is considered as a Lambertian surface with a solar reflection coefficient of ρ_g and the horizon is assumed unobstructed.

Similarly, the hourly global solar radiation on a horizontal surface (I_H) is the sum of the beam ($I_{H,b}$) and diffuse solar radiations ($I_{H,d}$)

$$I_H = I_{H,b} + I_{H,d} \tag{3}$$

Hence, relating the radiation on a tilted surface, Eq. (2), to that on a horizontal surface, Eq.(3), the hourly global solar radiation on a tilted surface, I_T, can be expressed as [14]:

$$I_T = I_{H,b} \cdot R_b + I_{H,d} \cdot \left(\frac{1+\cos\beta}{2} \right) + I_H \cdot \rho_g \cdot \left(\frac{1-\cos\beta}{2} \right) \tag{4}$$

where the geometric factor ($R_b \geq 0$) is the ratio of the beam solar radiation on the tilted surface ($I_{T,\,b}$) to the beam solar radiation on the horizontal surface ($I_{H,b}$). R_b is defined such as:

$$R_b = \frac{\cos\theta}{\cos\theta_z} = \frac{\cos(\phi-\beta)\cdot\cos\delta\cdot\cos\omega + \sin(\phi-\beta)\cdot\sin\delta}{\cos\phi\cdot\cos\delta\cdot\cos\omega + \sin\phi\sin\delta} \tag{5}$$

where the declination (δ) and the solar hour (ω) angles are given by [14]:

$$\delta = 23.45\sin\left(360\frac{284+n}{365} \right) \tag{6}$$

$$\omega = 15 \cdot (LST - 12) \tag{7}$$

Inserting Eq. (3) into Eq. (4) to eliminate the beam component $I_{H,b}$ and dividing by I_H leads to:

$$\frac{I_T}{I_H} = \left(1 - \frac{I_{H,d}}{I_H} \right) \cdot R_b + \frac{I_{H,d}}{I_H} \cdot \left(\frac{1+\cos\beta}{2} \right) + \rho_g \cdot \left(\frac{1-\cos\beta}{2} \right) \tag{8}$$

A critical solar radiation (hereafter I_c) is obtained when Eq. (8) is equal to 1. This study proposes that a "critical hourly global solar radiation" (I_c) can be defined as the hourly global solar radiation incident on the horizontal surface (I_H) for which the value is equal to the global solar radiation incident on a tilted surface (I_T). When I_H is below this threshold ($I_H < I_c$), a tilted surface would receive less energy than a horizontal one.

Then, for the condition $I_H = I_T = I_c$, the ratio of $I_{H.d} / I_c$ is calculated by modifying Eq. (8) as follows,

$$\frac{I_{H,d}}{I_c} = \frac{I_{H,d}}{I_H} = \frac{1 - \rho_g \cdot \left(\frac{1-\cos\beta}{2} \right) - R_b}{\left(\frac{1+\cos\beta}{2} \right) - R_b} \tag{9}$$

where, for a dual-axis tracking PV panel, cos θ=1, the geometric factor, R_b, simplifies to:

$$R_b = \frac{1}{\cos\phi \cdot \cos\delta \cdot \cos\omega + \sin\phi \sin\delta} \tag{10}$$

2.2. Correlation between solar radiation and clearness index

Orgill and Hollands [2] presented a correlation equation between the $I_{H.d} / I_H$ ratio and the hourly clearness index (k_t) based on Toronto's meteorological data collected over four years,

$$\begin{aligned} \frac{I_{H,d}}{I_H} &= 1 - 0.249 \cdot k_t & 0 \le k_t < 0.35 \\ \frac{I_{H,d}}{I_H} &= 1.557 - 1.84 \cdot k_t & 0.35 \le k_t \le 0.75 \\ \frac{I_{H,d}}{I_H} &= 0.177 & k_t > 0.75 \end{aligned} \tag{11}$$

The range $0 \le k_t < 0.35$ accounts for cloudy days with more than 90% of global incident solar radiation being diffuse. The range $0.35 \le k_t \le 0.75$ corresponds to partially sunny/cloudy days while sunny days are represented by $k_t > 0.75$.

Rewriting Orgill and Hollands [2] correlations and considering that $I_H = I_c$, the critical hourly clearness index for cloudy and partly sunny/cloudy days can be estimated as:

$$\begin{aligned} k_{t_c} &= \frac{1 - \frac{I_{H,d}}{I_c}}{0.249} & \frac{I_{H,d}}{I_c} > 0.91 \\ k_{t_c} &= \frac{1.557 - \frac{I_{H,d}}{I_c}}{1.84} & 0.177 \le \frac{I_{H,d}}{I_c} \le 0.91 \end{aligned} \tag{12}$$

Finally, the critical hourly solar radiation on a horizontal surface (I_c) can be estimated using,

$$I_c = k_{t_c} \cdot I_{H,0} \tag{13}$$

where the extraterrestrial solar radiation on a horizontal surface ($I_{H,0}$) for an hour period between hour angles ω_1 and ω_2 ($\omega_2 > \omega_1$) is given by [14]:

$$\begin{aligned} I_{H,0} = & \frac{12 \cdot G_{sc}}{\pi} \cdot \left[1 + 0.033 \cos\left(\frac{360 \cdot n}{365} \right) \right] \\ & \times \left[\cos\phi \cdot \cos\delta \cdot \left(\sin\omega_2 - \sin\omega_1 \right) + \frac{\pi \cdot \left(\omega_2 - \omega_1 \right)}{180} \cdot \sin\phi \cdot \sin\delta \right] \end{aligned} \tag{14}$$

The definition, Eq.(13), of the hourly I_c in conjunction with Eq.(14), will be used to determine whether or not a PV panel should track the sun for each hour a given day.

2.3. The number of cloudy days per month in Toronto

To assess the overall impact of the tracking strategy, first it is necessary to know the monthly fraction of cloudy days, k_t<0.35 or f(0.35), in Toronto (43.67° N 79.4° W). The following correlations employed by Duffie and Beckman [14] were used to assess the frequency of occurrence of overcast days per month:

$$f(0.35) = \frac{e^{(\gamma \cdot K_{T,min})} - e^{(\gamma \cdot 0.35)}}{e^{(\gamma \cdot K_{T,min})} - e^{(\gamma \cdot K_{T,max})}} \tag{15}$$

where

$$\xi = \frac{K_{T,max} - K_{T,min}}{K_{T,max} - \overline{K}_T} \tag{16}$$

$$\gamma = -1.498 + \frac{1.184 \cdot \xi - 21.182 \cdot e^{(-1.5 \cdot \xi)}}{K_{T,max} - K_{T,min}} \tag{17}$$

and

$$K_{T,max} = 0.6313 + 0.267 \cdot \overline{K}_T - 11.9 \cdot (\overline{K}_T - 0.75)^8 \tag{18}$$

The monthly average clearness index ($\overline{K}_T$) is the ratio of monthly average radiation on a horizontal surface to the monthly average daily extraterrestrial radiation. As in Duffie and Beckman [14], a minimum daily clearness index value corresponding to heavily overcast days ($K_{T,min}$) of 0.05 was used. The frequency of occurrence of overcast days per month is represented by $f(0.35)$, Eq. (15), and this value is reported in Table 1. The monthly average radiation impinging on a horizontal surface in Toronto was obtained from the PV-Sol Pro 4.5's meteorological database.

Table 1. Monthly fraction of cloudy days in Toronto

Months	$\overline{K}_T$	$K_{T,max}$	ξ	γ	*f(0.35)*	Overcast days
January	0.41	0.74	2.08	0.33	0.27	8
February	0.45	0.75	2.32	1.22	0.25	7
March	0.47	0.76	2.48	1.73	0.23	7
April	0.49	0.76	2.61	2.09	0.22	7
May	0.51	0.77	2.80	2.55	0.20	6
June	0.54	0.78	3.07	3.13	0.18	5
July	0.56	0.78	3.31	3.61	0.17	5
August	0.53	0.77	3.02	3.04	0.19	6
September	0.50	0.77	2.73	2.39	0.21	6
October	0.45	0.75	2.35	1.33	0.24	7
November	0.35	0.72	1.83	-0.84	0.30	9
December	0.35	0.72	1.80	-1.03	0.31	10

Table 1 shows that in Toronto there is at least one week per month of overcast days that is $0.17 < f(0.35) < 0.31$. In winter, up to a third (31%) of a month can be overcast.

2.4 Critical hourly global solar radiation of a two axis tracking system

The calculation of the critical hourly global solar radiation for a two axis solar tracking PV panel operating in Toronto was performed using the method described in the previous section. The calculations were made considering a ground reflection coefficient value of 0.2 for the summer season (June, July, August) and values of 0.2 (without ground snow coverage) and 0.8 (with snow on the surrounding ground) for the winter season (December, January, February).

Fig. 1 illustrates the critical hourly solar radiation (I_c) values in summer and winter. For levels of global solar radiation incident on a horizontal plane below these critical radiation values, the PV panel should receive more solar energy in a horizontal position. It is important to clarify that the solar radiation value is valid for the hour ending at the time indicated on the abscissa.

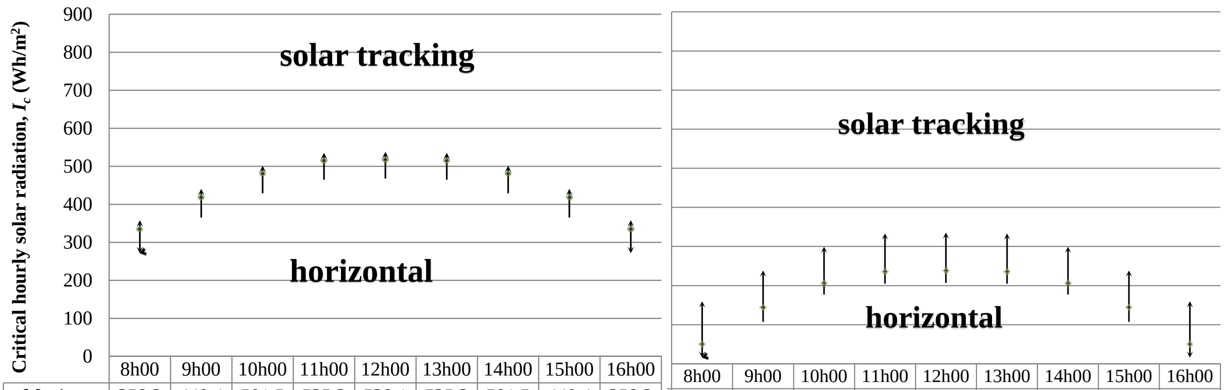

	8h00	9h00	10h00	11h00	12h00	13h00	14h00	15h00	16h00
Maximum	358,3	440,4	501,5	535,3	538,1	535,3	501,5	440,4	358,3
Minimum	271,4	356,4	420,5	456,1	459,0	456,1	420,5	356,4	271,4
Average	334,8	418,2	480,5	515,0	517,8	515,0	480,5	418,2	334,8

	8h00	9h00	10h00	11h00	12h00	13h00	14h00	15h00	16h00
Maximum	159,7	238,5	299,1	333,0	335,6	333,0	299,1	238,5	159,7
Minimum	15,9	99,5	169,0	197,1	198,9	197,1	169,0	99,5	15,9
Average	50,8	144,2	206,1	236,1	238,1	236,1	206,1	144,2	50,8

(a) (b)

Fig.1. Critical solar radiation for Toronto during : (a) summer (June, July, August); (b) winter (Dec., Jan., Feb.), ρ_g=0.2.

In Fig. 1a, the maximum values are observed for the summer solstice and the minimum values for the last days of August. In Fig. 1b, the maximum values show up in the last days of February and the minimum values at the winter solstice. The maximum value of the critical hourly solar radiation occurs at solar noon and this ranges from 238 Wh/m^2 (winter season) to 518 Wh/m^2 (summer season).

In Toronto, as in many other Canadian cities, cloudy winter days often coincide with snowfall. Snow significantly impacts the horizontal PV panel performance. On the other hand, the snow on the ground increases the component of the reflected radiation and this leads to a considerable reduction of the critical solar radiation. Table 2 shows that snow on the ground reduces the hourly average I_c almost by a factor of 3.

Table 2. Albedo's influence on average critical solar radiation for Toronto in winter.

Albedo	8h00	9h00	10h00	11h00	12h00	13h00	14h00	15h00	16h00
ρ_g=0.2	50.8	144.2	206.1	236.1	238.1	236.1	206.1	144.2	50.8
ρ_g=0.8	12.7	40.6	69.8	89.5	93.3	89.5	69.8	40.6	12.7

Such a decrease in the value of the critical solar radiation, I_c, caused by snow could make it advantageous to track the sun path even in cloudy conditions..

Now, as the threshold for $I_H = I_T = I_c$ is very low, even when the incident solar radiation on the horizontal plane, I_H, during a cloudy day is below the critical solar radiation, I_c, the advantage of producing electricity by fixing the PV panels horizontally has to be demonstrated. At such low levels of solar radiation, the PV photosensitive properties (current-voltage characteristic curve) and the operating parameters of the other PV system components (charge regulator, electric battery, and inverter) may provide significant constraints to the transformation of the incident solar energy into useful electrical energy. Hence, it is mandatory to compare the above conclusions with the electricity production of a panel.

3. Case study for a grid connected PV system

PV-Sol Pro 4.5 [15] was used to analyse the performance of a typical grid-connected PV system operating under cloudy sky conditions. To carry out the simulation, a PV system connected to Toronto's electrical grid was chosen. The system has a total power of 10.8kW and is composed of 48 PV panels of 225W each (Type PV panel: CS6P-225P) and 3 inverters (Inverter type: Powador 5300). Similar ground reflection coefficients were used.

In the supplied climate files of this software, radiation to the horizontal plane is given in Watt per square meter of active solar surface (radiation to the horizontal plane). The software uses the anisotropic sky model proposed by Hay and Davies [16], to estimate hourly solar radiation incident on a tilted surface (I_T). The diffuse solar radiation coming from the circumsolar area is projected onto the tilted surface in the same manner as the direct sunlight. Therefore, the ratio of the diffuse solar radiation on a tilted surface to the diffuse solar radiation on the horizontal surface, R_d, is given by

$$R_d = \left[(1 - A_i) \cdot \left(\frac{1 + \cos\beta}{2} \right) + A_i \cdot R_b \right] \quad (19)$$

Hay and Davies [16] defined an anisotropic index (A_i) for weighting the circumsolar and isotropic radiation components.

$$A_i = \frac{I_{H,b}}{I_{H,0}} \quad (20)$$

For cloudy sky conditions, the anisotropic model approaches the isotropic model, $A_i \approx 0$.

PV-Sol Pro 4.5 assumes that the PV modules are operated in maximum power point (MPP) operation. It determines the actual power output of these modules from the power output that they would provide under standard test conditions and from their efficiency characteristic curves. The software checks at every calculation step whether the module MPP voltage can be set by the inverter in order to simulate the MPP tracking of the inverter. If the MPP voltage is outside the MPP tracking range of the inverter, or if several arrays are connected to one inverter with different MPP voltages, the controller lowers the I-V characteristics of the modules until the working point has been found at which the maximum output can be obtained from the PV array [15].

To evaluate the solar tracking advantage (TA), a correlation similar to Eq. (1) was used. In this equation, instead of using values of hourly incident solar irradiance, values of hourly electrical energy produced by the solar tracking PV panels (E_{DTS}) and the horizontally oriented PV panels (E_H) are employed.

$$TA_{H,net} = \frac{E_{DTS} - E_H}{E_H} \quad (21)$$

In this respect, Eq. (1) can be considered to correspond to a "rough" tracking advantage based upon the radiation that strikes the panel, while Eq. (21) indicates a "net" tracking advantage based on the energy production.

In Tables 3, 4 and 5, the column labeled "I_c" represents the calculated hourly values of critical solar radiation for the specific day. The columns "I_H", "E_{DTS}" and "E_H" indicate the values of hourly global solar radiation incident on the horizontal surface, the values of hourly electrical energy produced by the solar tracking PV panels and the horizontally placed PV panels, respectively, obtained from the simulation carried out with PV-Sol Pro 4.5. The last column indicates net tracking advantage of solar tracking in percentage. Two cloudy days close to the summer solstice (Table 3, June 17th) and winter solstice (Tables 4 and 5, December 26th) were chosen for analysis.

Table 3 confirms that for levels of hourly global solar radiation incident on a horizontal surface below the critical solar radiation and a ground reflection coefficient equal to 0.2, the tracking mechanism should drive solar PV panels in a horizontal position. For every hour in Table 3, I_H is lower than I_c while the calculated tracking advantage is negative. The results show that when the ratio I_H/I_c is below about 60% there should not be tracking. In this case study, 8.8% less electrical energy would be generated if the system maintains the solar tracking for one cloudy day, neglecting the energy consumption of the tracking motors. As indicated in the table, this effect is more noticeable at sunrise and sunset, due to the inclination of the PV panels (60° to 80°) for these periods of the day. When the PV panels are approaching the zenith position, the effect is greatly reduced, since the panels adopt a less inclined position (between 20° and 30°). Results presented for this typical day are representative of any cloudy summer day.

Table 3. Net tracking advantage for a cloudy day close to the summer solstice (June 17th).

LST	I_c (Wh/m^2)	I_H (Wh/m^2)	E_{DTS} (Wh)	E_H (Wh)	$TA_{H,net}$ (%)
04:00	0.0	0.5	0.0	0.0	0.0
05:00	38.4	27.5	0.0	60.8	-100.0
06:00	167.7	79.9	421.5	688.1	-38.7
07:00	263.9	136.0	1021.9	1232.0	-17.1
08:00	358.1	192.5	1560.0	1773.9	-12.1
09:00	440.3	234.0	1993.7	2165.8	-7.9
10:00	501.5	284.6	2524.3	2642.3	-4.5
11:00	535.3	308.3	2794.0	2866.5	-2.5
12:00	538.1	307.4	2785.7	2845.9	-2.1
13:00	535.3	296.9	2653.0	2739.4	-3.2
14:00	501.5	259.6	2249.1	2385.6	-5.7
15:00	440.3	221.8	1841.3	2033.6	-9.5
16:00	358.1	165.3	1282.7	1497.1	-14.3
17:00	263.9	106.9	752.5	935.1	-19.5
18:00	167.7	48.3	84.6	213.8	-60.4
19:00	38.4	4.0	0.0	0.0	0.0
Total value	4729.2	2673.4	21964.2	24079.6	-8.8

Table 4. Net tracking advantage for a cloudy day close to the winter solstice (December 26th, ρ_g = 0.2).

LST	I_c (Wh/m^2)	I_H (Wh/m^2)	E_{DTS} (Wh)	E_H (Wh)	$TA_{H,net}$ (%)
08:00	16.7	15.0	0.0	0.0	0.0
09:00	101.3	47.2	180.9	340.4	-46.8
10:00	170.3	73.1	421.0	717.0	-41.3
11:00	198.4	106.9	874.0	1089.7	-19.8
12:00	200.3	80.6	601.7	790.2	-23.9
13:00	198.4	87.3	665.0	866.2	-23.2
14:00	170.3	75.8	575.8	734.4	-21.6
15:00	101.3	45.3	189.1	227.2	-16.8
16:00	16.7	3.7	0.0	0.0	0.0
Total value	1173.7	534.9	3507.6	4765.0	-26.4

Table 4 shows an increased disadvantage of solar tracking during cloudy winter days when ρ_g = 0.2. In this case, the PV panels would generate 26.4% less electrical energy if the system retains the solar tracking strategy. This could represent a significant penalty for electricity production during the shortest days having the lowest solar radiation. In winter months, the tracking disadvantage is more homogeneous during the day, because the PV panels field of view always contains a large fraction of ground due to its high inclination (60° to 80°) all day. Here again, the concept of critical solar radiation proposes similar conclusions that is for every hour ($I_H < I_c$) suggesting that the panels should be horizontally oriented.

The above results can be explained by the fact that during cloudy days, the solar radiation scattered by the atmosphere and clouds, and reflected from the ground represents a much larger fraction of the total irradiation. Moreover, for small values of ground reflection coefficient the diffuse solar radiation coming from the sky dominates and its intensity depends on the fraction of the sky seen by the PV panel. For this reason, the horizontal position offers the best performance. On the other hand, when the albedo is high due to the presence of the snow on the ground, the situation is completely different as shown in Table 5 for $\rho_g = 0.8$.

Table 5. Net tracking advantage for a cloudy day close to the winter solstice (December 26th, $\rho_g = 0.8$).

LST	I_c (Wh/m^2)	I_H (Wh/m^2)	E_{DTS} (Wh)	E_H (Wh)	$TA_{H,net}$ (%)
08:00	4.1	15.0	0.0	0.0	0.0
09:00	25.2	47.2	341.8	340.4	0.4
10:00	49.7	73.1	708.1	717.0	-1.2
11:00	66.7	106.9	1098.9	1089.7	0.8
12:00	70.1	80.6	763.8	790.2	-3.3
13:00	66.7	87.3	857.0	866.2	-1.1
14:00	49.7	75.8	753.2	734.4	2.6
15:00	25.2	45.3	353.6	227.2	55.7
16:00	4.1	3.7	0.0	0.0	0.0
Total value	361.5	534.9	4876.3	4765.0	2.3

Table 5 shows a slight solar tracking advantage of 2.3% when $\rho_g = 0.8$. Here the use of the I_c concept could be challenged as (I_H) is always higher than (I_c) thus indicating that for every hour the system should track the sun. However, although there might be an advantage based on the amount of energy that strikes the panel, when operating parameters and losses are accounted for, this advantage is found to be much less or inexistent.

Despite this remark, overall these results confirm those reported in Table 2, where a decrease in the critical solar radiation value caused by the increase of albedo permitted to anticipate the advantage of tracking the sun path even on cloudy days. On those days the penalty associated with the observation of the ground is minimal because it reflects diffuse radiation. In consequence, it is advantageous to optimise the collection of the residual direct solar radiation. Nevertheless, one should note that the overall gains are small in relative and in absolute terms, and close to the energy consumption reported for some tracking systems [17-21]. Results for 15:00 indicate a major discrepancy with other results: this indicates that close to sunset that day, the cloud cover was not uniform or constant. At that time of the day in winter, there is much more direct sunlight that strikes a tracking surface than a horizontal one.

The former issue led to the analysis of a third strategy, characterized by leaving the PV panels fixed in a tilted position. The analysis was performed for a PV array tilted at 57°. The results (not reported here) show a slight advantage of 0.8% for the PV tilted system with respect to the solar tracking system. This could suggest that on a cloudy day with snow on the ground the PV panels could remain in a south-facing tilted position without affecting the electricity production and without unnecessary electrical consumption required to operate the motors.

4. Proposed tracking strategy

Fig. 2 is an attempt to summarize the tracking strategies analysed for a solar PV system operating in Canada or any high latitude area involving snow falls for cloudy days based on the above-mentioned results. Fig. 2 first indicates that when the sky is either clear or only partly sunny/cloudy ($I_H > I_c$), the tracker should work normally. For overcast days ($I_H \leq I_c$) without either snowfall or snow on the ground, the tracker should put the collector horizontally. Now, when there is either some snow falling or snow on the ground, the collector should still be left in a fixed position but this time with the optimal tilt angle for the location.

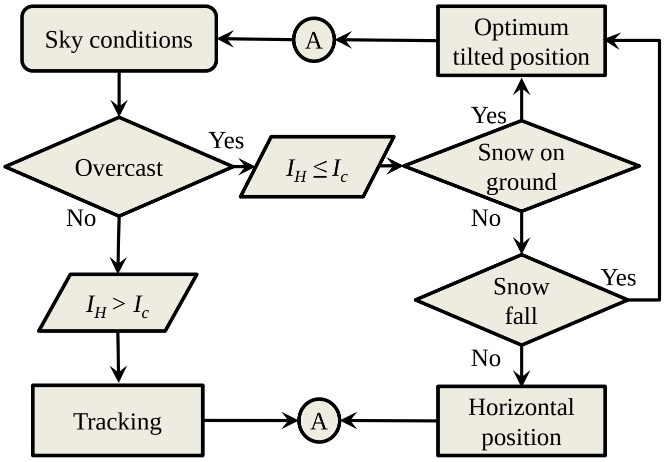

Fig.2. Schematic of the control strategy for a mobile PV solar panel based on the prediction of the hourly solar radiation

Figure 2 indicates that tracking is the optimal strategy as soon as the sky is clear or only partly cloudy. This means that the versatility of the tracking systems to adopt different solar tracking strategies – seeking to maximize electricity production for each environmental condition – could rely on the knowledge of local weather conditions, which leads to the idea of developing a predictive command system based on weather forecasts.

5. Conclusion

The main goal of this study was to find the optimum tracking strategy for cloudy conditions in Canada or any high latitude location. To clarify this issue, the solar energy availability and the transformation of this solar energy into electricity using a dual-axis solar tracker PV panel were analyzed separately under climate conditions of Toronto, Canada.

5.1 Critical hourly solar radiation

A methodology to estimate a theoretical threshold – the critical hourly solar radiation – below which the PV panel in a horizontal position receives more energy than following the sun was developed. The critical solar radiation values were established near the limit zone that separates the partially sunny/cloudy days and the cloudy days. Hence, for levels of global solar radiation incident on a horizontal plane below these critical radiation values (overcast days), the dual-axis solar tracker PV panel energy performance can be improved by setting the PV panel in a horizontal position. However, during the winter season, snow on the ground increases the albedo and this reduces the critical solar radiation, making it advantageous to track the sun path, even on cloudy days. The proposed methodology will be used in future work to evaluate the PV solar tracking advantages in different locations across Canada by applying the concept of monthly average daily utilizability reported by Duffie and Beckman [14].

5.2 Electricity production

The analysis of case studies on the transformation of solar energy into electricity confirms the sun tracking disadvantage on cloudy days in summer. This occurs when levels of global solar radiation incident on a horizontal plane (I_H) are below the critical radiation values (I_c). However, on a cloudy winter day, the strategy of solar tracking, keeping the PV panel in a tilted position or bringing the PV panel up to a horizontal position, depends on the snow presence on the ground.

The experimental validation [10] of this theoretical study was carried out for another Canadian location, Montreal. These papers result from the initial phase of an ongoing project aimed to developing a predictive control system based on weather forecast.

Acknowledgments

The authors gratefully acknowledge the Natural Sciences and Engineering Research Council of Canada (NSERC) for financial support. The authors also thank the partners of the t3e research chair who support the project.

Nomenclature

A_i	anisotropic index
E	hourly electrical energy produced by the solar PV array (Wh)
R	effective ratio of solar energy on a tilted surface to that on a horizontal surface
G	solar irradiance on a surface (W/m^2), in Kelly and Gibson [5]
G_{sc}	extraterrestrial solar irradiance, solar constant = 1353 W/m^2
I	hourly solar radiation (Wh/m^2)
k_t	hourly clearness index
K_T	daily clearness index
$\overline{K}_T$	monthly average clearness index
LST	local solar time
n	nth day of the year
R_b	geometric factor
R_d	geometric factor
TA	tracking advantage

Greek symbols

β	surface slope (°)
δ	solar declination (°)
ξ, γ	dimensionless parameters used in Eq.(21)
ω	solar hour angle (°)
Φ	latitude (°)
ρ_g	ground reflection coefficient
θ	incidence angle (°)
θ_z	zenith angle (°)

Subscripts

0	extraterrestrial
b	direct beam
c	critical
d	diffuse
DTS	pointing directly toward the sun
H	horizontally oriented
r	reflected
T	tilted or inclined
T-57°	tilted 57°

References

[1] Mousazadeh H., Keyhani A., Javadi A., Mobli H., Abrinia K., Sharifi A., A review of principle and sun-tracking methods for maximizing solar systems output. Renewable and Sustainable Energy Reviews 2009; 13, 1800–1818.

[2] Orgill J.F., Hollands G.T.,. Correlation equation for hourly diffuse radiation on a horizontal surface. Solar Energy 1977; 19, 357-359.

[3] Appelbaum J., Flood D.J., Crutchik M., Solar radiation on mars: tracking photovoltaic array. NASA Technical Memorandum 106700, 1994.

[4] Badescu V., Simulation of solar cells utilization on the surface of Mars. Acta Astronautica 1998; 43, 443-453.

[5] Kelly N.A., Gibson T.L., Improved photovoltaic energy output for cloudy conditions with a solar tracking system. Solar Energy 2009; 83, 2092–2102.

[6] Kelly N.A., Gibson T.L., Increasing the solar photovoltaic energy capture on sunny and cloudy days. Solar Energy 2011; 85, 111–125.

[7] Koussa M., Cheknane A., Hadji S., Haddadi M., Noureddine S., Measured and modeled improvement in solar energy yield from flat plate photovoltaic systems utilizing different tracking systems and under a range of environmental conditions. Applied Energy 2011; 88, 1756–1771.

[8] Koussa M., Haddadi M., Saheb D., Malek A., Hadji S., Sun tracking mechanism effects on flat plate photovoltaic system performances for different step time and main parameters affecting the obtained gains: case of North Africa and Mediterranean site. Energy Procedia 2012; 18, 817 – 838.

[9] Koussa M., Haddadi M., Saheb D, Malek A. Hadji S., Sun tracker systems effects on flat plate photovoltaic PV systems performance for different sky states: A case of an arid and hot climate. Energy Procedia 2012; 18, 839 – 850.

[10] Guillon L., Quesada, G., Rousse D.R., A tracking strategy for a photovoltaic solar system in high latitudes. Submitted to Energy Conversion and Management, 2015

[11] Hay J.E., McKay D.C., Estimating solar irradiance on inclined surfaces: a review and assessment of methodologies. International Journal of Solar Energy 1985; 3, 203-240.

[12] Reindl D.T., Beckman W.A., Duffie J.A., Evaluation of hourly tilted surface radiation models. Solar Energy 1990; 45, 9-17.

[13] Noorian A.M., Moradi I., Kamali G.A., Evaluation of 12 models to estimate hourly diffuse irradiation on inclined surfaces. Renewable Energy 2008; 33, 1406-1412.

[14] Duffie J.A., Beckman W.A., Solar engineering of thermal processes. John Wiley & Sons Inc., Hoboken, New Jersey; 2006.

[15] Valentin, 2010, http://valentin-software.com/products/photovoltaics, [accessed 11.09.2014].

[16] Hay J.E., Davies J.A., Calculation of the solar radiation incident on an inclined surface. Proceedings First Canadian Solar Radiation Data Workshop, 1980; 59-72.

[17] Abdallah S., Nijmeh S., Two axes sun tracking system with PLC control. Energy Conversion and Management 2004; 45, 1931–1939.

[18] Abu-Khader M.M., Badran O.O., Abdallah S., Evaluating multi-axes sun-tracking system at different modes of operation in Jordan. Renewable and Sustainable Energy Reviews 2008; 12, 864–873.

[19] Mamlook R., Nijmeh S., Abdallah S.M., A programmable logic controller to control two axis sun tracking system. Information Technology Journal 2006; 5, 1083–1087.

[20] Poulek V., Testing the new solar tracker with shape memory alloy actors. Conference Record of the Twenty Fourth IEEE Photovoltaic Specialists Conference 1994; 1, 1131–1133.

[21] Poulek V., Libra M., New solar tracker. Solar Energy Materials and Solar Cells 1998; 51, 113–120.